Surface-directed spinodal decomposition: modelling and numerical simulations

1997 J. Phys.: Condens. Matter 9 2109

(http://iopscience.iop.org/0953-8984/9/10/003)

J. Phys.: Condens. Matter **9** (1997) 2109–2133. Printed in the UK PII: S0953-8984(97)67977-1

REVIEW ARTICLE

Surface-directed spinodal decomposition: modelling and numerical simulations

Sanjay Puri†‡ and Harry L Frisch‡§

† School of Physical Sciences, Jawaharlal Nehru University, New Delhi-110067, India
‡ Institut fur Physik, Johannes Gutenberg-Universitat Mainz, D-55099 Mainz, Germany
§ Department of Chemistry, State University of New York at Albany, 1400 Washington Avenue, Albany, NY 12222, USA

Received 19 November 1996

Abstract. We critically review the modelling and simulations of surface-directed spinodal decomposition, namely, the dynamics of phase separation of a critical or near-critical binary mixture in the presence of a surface with a preferential attraction for one of the components of the mixture.

1. Introduction

Multicomponent mixtures are of considerable technological and scientific relevance and there have been many studies focusing on the thermodynamic properties of mixtures. More recently, attention has turned to problems of phase-ordering dynamics, i.e., the temporal evolution of a homogeneous two-phase mixture which has been rendered thermodynamically unstable by a rapid pressure or temperature quench [1]. Typically, the unstable mixture (say, AB) decomposes into A- and B-rich domains which coarsen with time. For pure and isotropic systems, the coarsening domains are characterized by a unique time-dependent length scale $L(t)$, where t is the time. An important consequence of the existence of this unique length scale is the dynamical scaling of the order parameter correlation function $g(\boldsymbol{r}, t) = \langle \phi(\boldsymbol{R}, t)\phi(\boldsymbol{R}+\boldsymbol{r}, t)\rangle$, where $\phi(\boldsymbol{R}, t)$ is the order parameter at point $\boldsymbol{R}$ and time t, and the angular brackets denote an averaging over independent initial conditions. The dynamical scaling property states that $g(\boldsymbol{r}, t)$ only depends on time t through a scale factor for the distance variable [2], i.e.,

$$g(\boldsymbol{r}, t) = G(r/L(t)) \tag{1}$$

where $G(x)$ is a time-independent master function. In more physical terms, dynamical scaling of the correlation function implies that the coarsening domain morphology is self-similar in time.

The primary interest of most studies in phase-ordering dynamics has been to elucidate the nature of the asymptotic domain growth law and the functional form of the correlation function $G(x)$ or its momentum-space counterpart. For pure and isotropic systems characterized by a scalar order parameter, there is now a good understanding of these properties—at least experimentally and numerically [1]. Thus, it is well established that the asymptotic length scale exhibits a power-law behaviour $L(t) \sim t^{\phi}$, where ϕ is referred to as the growth exponent. The value of this exponent depends critically on whether or not the

0953-8984/97/102109+25$19.50

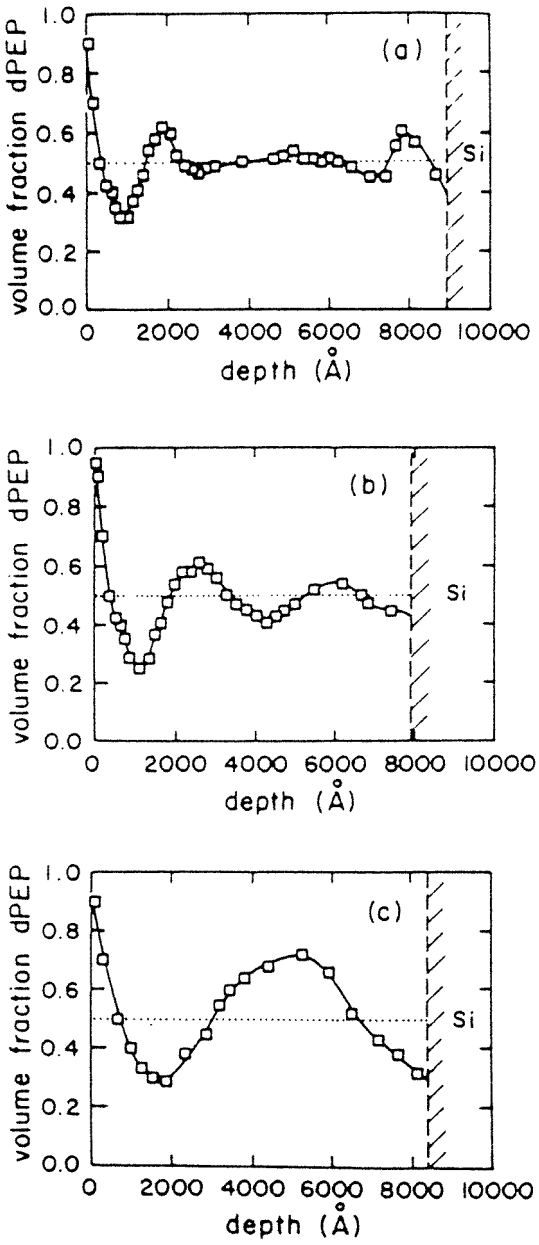

Figure 1. The volume fraction of d-PEP as a function of depth for surface-directed spinodal decomposition in critical polymer mixtures of PEP and d-PEP [6]. These profiles were obtained by a lateral averaging (parallel to the surface) of spinodal decomposition waves, which are randomly oriented in the bulk but not near the surface. The surface has a preferential attraction for d-PEP and is located at zero depth. Order parameter profiles are shown for times corresponding to: (a) 19 200 s; (b) 64 440 s; and (c) 172 800 s. (From reference [6].)

evolution is characterized by a conserved order parameter. Thus, $\phi = 1/2$ for the case of a ferromagnet undergoing an ordering transition, where the order parameter (i.e., spontaneous magnetization) is not conserved. Furthermore, $\phi = 1/3$ for the case of a phase-separating binary mixture AB in the absence of hydrodynamic effects. In this case, the order parameter (i.e., the local difference in densities of A and B) is conserved. The above growth laws are usually referred to as the Lifshitz–Cahn–Allen (LCA) and Lifshitz–Slyozov (LS) laws, respectively. The case of a phase-separating binary fluid is more involved because of the coupling of the conserved order parameter (i.e., the density field) to the hydrodynamic velocity field, which plays an important role in the late stages of phase separation [3]. The growth exponent for segregating binary fluids depends on the dimensionality and also the particular regime of interest [4].

Recent attention in the area of phase-ordering dynamics has turned to experimentally realistic systems and the incorporation of experimentally relevant effects into traditional idealized models. The present article reviews theoretical and numerical developments for a particularly interesting problem in this class, i.e., the behaviour of phase-separating binary mixtures in the presence of a surface which has a preferential attraction for one of the components of the mixture. Theoretical interest in this problem has been motivated by a number of beautiful experiments, many of which have been recently reviewed by Krausch [5]. We will primarily focus on homogeneous binary mixtures which have been quenched into a region of the phase diagram where they are unstable and undergo spontaneous phase separation or spinodal decomposition in the bulk. Of course, the situation in which the binary mixture has a highly off-critical composition and separates via nucleation and growth is also of great experimental and theoretical interest. However, this situation has received considerably less attention so far and we will not focus on it here.

This paper is organized in the following fashion. In section 2, we provide a brief overview of some experiments which have motivated theoretical interest in surface-directed spinodal decomposition. Section 3 critically examines various models of this phenomenon and the numerical results obtained from these models. Section 4 concludes this paper with a summary and discussion.

2. A brief overview of the experimental results

In this paper, we present only a brief overview of some relevant experiments in the study of surface-directed spinodal decomposition. As we have remarked earlier, an extensive review of the extant experimental situation has already been provided by Krausch [5] and we refer the interested reader to that paper.

To the best of our knowledge, the first relevant experimental study of this problem is due to Jones *et al* [6], who studied the spinodal decomposition of critical mixtures of poly(ethylenepropylene) (PEP) and perdeuterated poly(ethylenepropylene) (d-PEP) in the presence of a surface with a preferential attraction for d-PEP. (Their experiment was motivated by the theoretical work of Ball and Essery [7], which we will discuss in the next section.) Jones *et al* observed that the surface became the origin of composition waves with wave-vectors normal to the surface and propagating into the bulk, as depicted in figure 1. They referred to these waves as 'surface-directed spinodal decomposition waves'. Apart from these qualitative observations, the initial experiments of Jones *et al* [6] were unable to make clear quantitative statements about the temporal evolution of these waves and associated domain growth phenomena.

Krausch *et al* [8] improved on these first experiments, using a similar experimental system but with better techniques. Their results indicated that the surface-directed spinodal

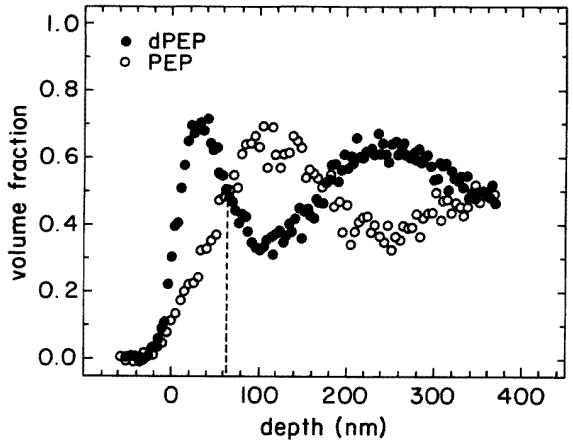

(a)

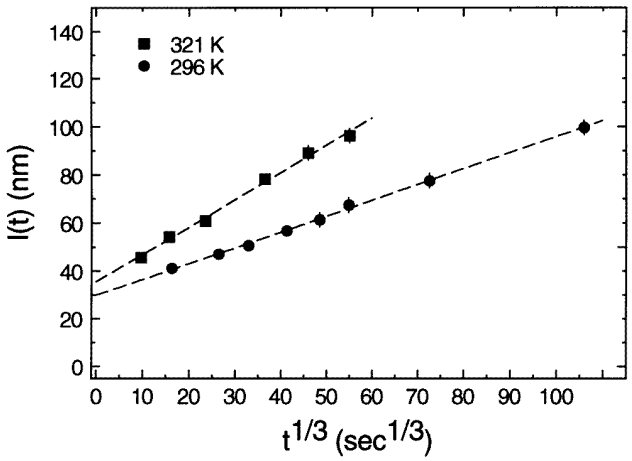

(b)

Figure 2. (a) Typical volume fraction profiles for d-PEP and PEP as a function of depth in critical polymer mixtures of PEP and d-PEP phase separating near a surface with a preference for d-PEP. These experimental results were obtained by Krausch *et al* [8] and correspond to a time of 14 400 s after the quench. To compare these profiles with those of Jones *et al* [6] in figure 1, the 'pre-surface' region up to about 20 nm should be discarded. (From reference [8].) (b) The time dependence of the first zero of the volume fraction profiles shown in figure 2(a). The first zero (denoted as $l(t)$ here) is plotted versus $t^{1/3}$ (t being the time) for two different quench depths. The dashed lines correspond to linear best fits. These experiments correspond to the limit of weak surface field and high thermal noise and the corresponding domain morphology is partially wet, with domains of both phases being in contact with the surface. (From reference [8].)

decomposition waves penetrated into the bulk in a power-law fashion; and the first zero crossing, $R_1(t)$, of these profiles obeyed the LS growth law $R_1(t) \sim t^{1/3}$ (see figure 2). Their experiments were also motivated, in part, by the numerical studies of Brown and Chakrabarti [9] and Marko [10], which we will summarize in the next section. However, we would like to stress that the experimental situation of Krausch *et al* in reference [8] corresponds to a

situation in which the surface field is weak compared to thermal noise, so the surface is only partially wetted by droplets of the preferred phase. A similar situation was also studied by Straub *et al* [11] using critical polymer mixtures of deuterated polystyrene (dPS) and partially brominated polystyrene (PBr_xS). These authors found that that the preferred phase initially formed a plated layer at the surface, which grew out for a while before decomposing into a partially wet morphology with domains of both phases in contact with the surface. The layer thickness (defined from the first zero of the laterally averaged profiles) again obeyed the LS growth law $R_1(t) \sim t^{1/3}$.

One can also consider the opposite limit of a strong surface field and weak or no noise. In this situation, a multilayered structure rapidly forms at the surface. This structure consists of alternating layers of the preferred and non-preferred phases. The thickness of the layer of preferred phase at the surface grows at a rate which is determined by the nature of the forces exerted by the surface on the decomposing mixture. The strength of the surface field determines whether or not this layer wets the surface. We will elaborate further on this situation in the next section. Experimental realizations of this limit were studied by Krausch *et al* [12], who mimicked the low-noise situation by creating a multilayer of the coexisting phases of a binary polymer mixture (namely, dPS and PBr_xS) in contact with an unstable bulk. For early and intermediate times, they found that coarsening near the surface occurred by the dissolution of alternating layers of their initial structure. At late times, they again found results similar to those reported in reference [8]. It is not clear to us what the rather specialized experimental situation of Krausch *et al* [12] can say about general behaviour in the limiting case of strong field and weak noise.

A more recent experiment by Geoghegan *et al* [13] may be more relevant to this case. These authors studied surface-directed spinodal decomposition in blends of dPS and poly(α-methylstyrene) (PαMS). They report considerably slower growth of the surface layer than that seen in references [8] and [11] and it is possible that their experiment constitutes another realization of the low-noise limit.

As far as domain growth in the direction parallel to the surface is concerned, there have been a number of apparently conflicting observations. Again, it is appropriate to distinguish between two different physical situations. For example, in the case where domains of both phases are in contact with the surface, it is reasonable to examine the lateral domain growth at the surface itself. On the other hand, when the surface is completely covered by a thickening layer of the preferred phase, it is reasonable to consider lateral domain growth in the regions outside the systematic multilayered structure. (Of course, one can also consider the dynamics of fluctuations around the background value corresponding to the systematic profile at the surface.) The experiment of Straub *et al* [11] found that the lateral size of surface domains formed in the late stages of surface-directed spinodal decomposition in the low-field–high-noise limit obeys the LS growth law.

These results should be contrasted with the work of Wiltzius, Cumming and co-workers [14], who reported observations of a 'fast mode' of surface domain growth in their experiments on surface-directed spinodal decomposition in both polymer and binary fluid mixtures. They observed that the structure factor of the coarsening system exhibited two peaks rather than the single peak usually seen in bulk spinodal decomposition. The inverse position of the second peak (at larger wave-vectors) obeyed the appropriate bulk growth law (i.e., $L(t) \sim t$ or $L(t) \sim t^{1/3}$, depending on whether or not hydrodynamics is relevant), whereas the position of the first peak (at smaller wave-vectors) exhibited an anomalously fast growth law $L(t) \sim t^{\phi}$, with $\phi \sim 1.1$–1.5. Wiltzius *et al* interpreted this fast growth as an early-time regime in which a partially wet morphology evolves to one where the surface is completely covered by a continuous layer, which presumably grows

into the bulk at later times.

In our perception, the results of reference [14] should not be interpreted as being at variance with the results of Straub *et al* [11] because they correspond to different time regimes and physical situations. After all, the asymptotic state in the experiments of reference [11] corresponds to a partially wet surface with domains of both phases in contact with the wall—in contrast with the experiments of reference [14], where the fast mode precedes the formation of a continuous layer at the wall. Troian [15] has argued that this fast mode is the consequence of coalescence of domains of the non-wetting phase in contact with a continuous layer of the wetting phase of the surface. However, there are some ambiguities in her treatment. We are inclined to agree with Keblinski *et al* [16] that the extremely rapid formation of the wetting layer at the surface could be interpreted as corresponding to the fast mode reported in the experiments of Wiltzius, Cumming and co-workers [14].

Prior to the experiments of reference [14], Guenoun *et al* [17] had also studied the interplay of wetting and phase separation in binary fluid mixtures (cyclohexane and methanol) at critical concentrations. The time regime investigated by them corresponds to a situation in which the surface is already coated with a layer of the preferred phase. Guenoun *et al* [17] reported that domain growth perpendicular to the surface obeyed an asymptotic law consistent with that for the bulk, namely, $L(t) \sim t$. However, in contrast to the experiments of Wiltzius *et al* [14], they found that domain growth parallel to the surface was suppressed and, if a power-law fit were attempted, showed a growth exponent $\phi \sim 0.5$–0.7.

Tanaka [18] has also conducted experiments on binary polymer mixtures phase separating in one- or two-dimensional capillaries. Most of his experiments were conducted on mixtures of poly(vinylmethylether) (PVME) with water; or oligomer mixtures. Tanaka's primary focus was the interaction between phase separation and the wetting layer growing from the surface. In particular, he focused on the late stages of phase separation, where hydrodynamic effects dominate the segregation dynamics. Tanaka found a strong dependence of the evolution morphology on the composition of the mixture. As our primary interest is in the regime where hydrodynamic effects are not relevant, we do not present further details of Tanaka's work here but rather refer the interested reader to his original papers [18].

These representative experiments provide guidance to the relevant theoretical questions, which we would like to describe in the next section. Of course, development in this area has resulted from a symbiotic interaction between experiments, theory and numerical simulations. However, it is appropriate to summarize here the experimentally relevant features which must be manifested by any reasonable theoretical model for surface-directed spinodal decomposition. Modelling and simulations to date have so far been restricted to the case where hydrodynamic effects are not relevant. Therefore, we will only summarize experimental results for this situation. (In any case, there does not appear to be experimental unanimity on the behaviour of surface-directed spinodal decomposition in binary fluids.) It is experimentally clear that the attracting surface is rapidly enriched in the preferred component and becomes the source of anisotropic spinodal decomposition waves which propagate into the bulk perpendicular to the surface. The morphology of these waves and their temporal evolution depends critically on the relative strengths of the surface field and thermal noise, and on whether the surface field strength leads to a partial or complete wetting of the surface. However, domain growth parallel to the surface obeys the same asymptotic growth law as that in the bulk, except that there may be an enhanced domain growth near the surface due to the orientational effect of (partial or complete) wetting layers formed at the surface.

3. Theoretical modelling and numerical simulations

3.1. Early studies of surface-directed spinodal decomposition

One of the earliest analytical investigations of the effect of surfaces on spinodal decomposition is due to Xiong and Gong [19], who considered a semi-infinite Ising model characterized by a conserved scalar order parameter. In their model, the dynamics of the order parameter in the bulk obeys the usual Cahn–Hilliard–Cook (CHC) equation

$$\frac{\partial\phi(\boldsymbol{R}, Z, \tau)}{\partial\tau} = -\nabla^2\left[\phi(\boldsymbol{R}, Z, \tau) - \phi(\boldsymbol{R}, Z, \tau)^3 + \frac{1}{2}\nabla^2\phi(\boldsymbol{R}, Z, \tau)\right] + \eta(\boldsymbol{R}, Z, \tau) \qquad (2)$$

where $\phi(\boldsymbol{R}, Z, \tau)$ is the order parameter at space point $(\boldsymbol{R}, Z)$ and time τ, with $\boldsymbol{R}$ representing coordinates parallel to the surface and Z representing the coordinate perpendicular to the surface. (For consistency, we have already rescaled the CHC equation into the dimensionless form we will use throughout this paper.) In equation (2), $\eta(\boldsymbol{R}, Z, \tau)$ is a Gaussian white noise which obeys the appropriate fluctuation-dissipation theorem and it is assumed that the surface gives rise to a delta-function field, which does not penetrate into the bulk of the system. Xiong and Gong supplemented the bulk CHC equation with a boundary condition at the surface position $Z = 0$:

$$\left.\frac{\partial\phi(\boldsymbol{R}, Z, \tau)}{\partial Z}\right|_{Z=0} = C\phi(\boldsymbol{R}, 0, \tau) \qquad (3)$$

where C measures the strength of the delta-function field originating at the surface. Xiong and Gong used this model as the basis of an approximate theory for the time-dependent structure factor in the surface layer, following the treatment of Langer *et al* [20]. Their results indicated that phase separation in the boundary layer is faster than that in the bulk but they did not quantify the nature of domain growth near the surface. Unfortunately, the modelling of Xiong and Gong is open to criticism on two counts in the present context. Firstly, their model is incomplete without a second boundary condition at the surface, which would normally be of the 'no-flux' type, i.e.,

$$\left.\frac{\partial}{\partial Z}\left[\phi(\boldsymbol{R}, Z, \tau) - \phi(\boldsymbol{R}, Z, \tau)^3 + \frac{1}{2}\nabla^2\phi(\boldsymbol{R}, Z, \tau)\right]\right|_{Z=0} = 0 \qquad (4)$$

in conjunction with a corresponding condition on the thermal noise. Furthermore, the form of the surface free energy used by Xiong and Gong does not result in a preferential attraction of either of the components to the surface and is inappropriate in the context of surface-directed spinodal decomposition.

Jiang and Ebner [21] studied the effect of surfaces on phase separation through Monte Carlo (MC) simulations of a semi-infinite Ising model with Kawasaki spin-exchange kinetics. In their modelling, the surface preferentially attracted one of the components of a binary mixture. Jiang and Ebner studied cases with both short-ranged (delta-function) and long-ranged (power-law) surface potentials. They found that the thickness of the surface layer in their simulations always obeyed the LS growth law, regardless of the nature of the potential. However, their results for surface layer thickness exhibit a large degree of scatter and it is difficult to conclusively ascertain an asymptotic growth exponent from their data.

The next relevant study is due to Ball and Essery [7], who modelled surface-affected spinodal decomposition using equations (2)–(4). As we have remarked earlier, the boundary condition in equation (3) does not lead to surface-directed spinodal decomposition for critical quenches because the corresponding free energy does not discriminate between the two phases. For off-critical quenches, this model does exhibit symmetry breaking but

in a somewhat artificial fashion. Nevertheless, the pioneering work of Ball and Essery provided guidance to the initial experiments of Jones *et al* [6] on surface-directed spinodal decomposition. Furthermore, the initial study of Ball and Essery already recognised the important distinction between the multilayered morphology (arising in the high-field–low-noise case) and the partially wet morphology, in which domains of both phases were in contact with the wall (arising in the low-field–high-noise case).

In passing, we should also remark that Ball and Essery not only attempted to model the role of the boundary for the system (through appropriate boundary conditions), but also effects due to temperature gradients. This was done by directly coupling the temperature-dependent parameter implicit in the linear term of the CHC equation with a diffusion equation for the temperature field. Their description of this problem is also somewhat incomplete as there are additional terms coupling temperature and order parameter gradients which are missing in their model.

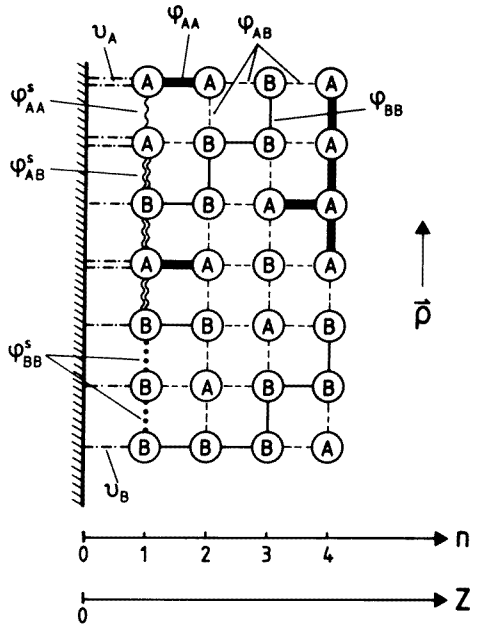

Figure 3. A schematic diagram of a binary alloy AB in contact with a surface located at layer $n = 0$ (or coordinate $z = 0$). We assume that there are only nearest-neighbour interactions and the different possible interactions are depicted on the figure. The energies associated with A–A (heavy line), B–B (light solid line), and A–B (dashed line) in the bulk are ϕ_{AA}, ϕ_{BB} and ϕ_{AB}, respectively. Our model also includes the possibility of different interactions in the surface layer ($n = 1$). Finally, we assume that the surface only interacts with the layer $n = 1$ via interactions ν_A and ν_B, though we can easily generalize to the case of long-ranged interactions [29]. (From reference [25].)

3.2. The dynamics of phase separation in a semi-infinite Ising model

In this subsection, we review our recent work on the modelling and simulation of surface-directed spinodal decomposition. As our primary interest was the interplay of wetting and spinodal decomposition, we have focused on the limit of high surface field and weak

thermal noise. Therefore, our numerical results are complementary to those of Brown and Chakrabarti [9] and Marko [10], which we present in the next subsection.

The phase separation of a binary mixture (say, AB) in the bulk can be described by an Ising-lattice model in which the constituents A and B may interchange directly via Kawasaki spin-exchange kinetics [22]. This is not a mechanistically realistic description of interdiffusion in solid alloys which usually depends on a vacancy-mediated mechanism nor that in fluid mixtures where hydrodynamic effects are relevant. Nevertheless, this microscopic model is a convenient starting point for motivating reasonable phenomenological models for phase separation. Binder [23] formulated a master equation approach to the kinetic Ising model which motivated the phenomenological Cahn–Hilliard (CH) equation starting from an Ising model with Kawasaki spin-exchange kinetics. Binder and Frisch [24] applied this approach to the semi-infinite Ising model with a delta-function surface field and Kawasaki kinetics. In the mean-field limit, they were able to obtain a coarse-grained model for surface-directed spinodal decomposition, which consisted of the CH equation in the bulk supplemented by two boundary conditions representing the surface. One of these boundary conditions was later modified by Puri and Binder [25], who explicitly incorporated the no-flux boundary condition of equation (4) into the model. Our discussion in this paper closely follows that of Puri and Binder. Ultimately, such a coarse-grained model is of more general validity than the particular lattice model used for its derivation and is expected to be applicable for every microscopic model in the same 'dynamical universality class' [26].

In our initial formulation, the surface forces were taken to be of delta-function form at the surface, because we felt that the simpler theory involving short-range forces must be understood first. The simple Ginzburg–Landau model with short-range surface forces has the advantage that its static limit, though highly non-linear, can be solved exactly [27, 28], allowing a detailed analysis of equilibrium wetting phenomena. In recent work [29], we have also incorporated long-ranged forces into our modelling and simulations and will discuss these briefly later.

3.2.1. The model Hamiltonian and formalism in the static case. The starting point of our modelling is a binary (AB) mixture in contact with a surface and with pairwise interactions ϕ_{AA}, ϕ_{AB}, ϕ_{BB} between atoms at sites $\boldsymbol{r}_i$ and $\boldsymbol{r}_j$, as is schematically depicted in figure 3. In terms of local concentration variables, $c_i = 1$ if site i is occupied by an A atom and $c_i = 0$ if it is occupied by a B atom. If the total number of atoms is N, the variable i ranges from 1 to N. The corresponding Hamiltonian is

$$\mathcal{H} = \sum_{i \neq j} [c_i c_j \phi_{AA}(\boldsymbol{r}_i, \boldsymbol{r}_j) + c_i(1 - c_j)\phi_{AB}(\boldsymbol{r}_i, \boldsymbol{r}_j) + (1 - c_i)c_j\phi_{AB}(\boldsymbol{r}_i, \boldsymbol{r}_j) + (1 - c_i)(1 - c_j)\phi_{BB}(\boldsymbol{r}_i, \boldsymbol{r}_j)] + \sum_i [\nu_A(\boldsymbol{r}_i)c_i + \nu_B(\boldsymbol{r}_i)(1 - c_i)] \tag{5}$$

where sums over pairs run over all pairs once, and lattice sites exist in the positive half-space $z > 0$ only. In equation (5), $\nu_A(\boldsymbol{r}_i)$ or $\nu_B(\boldsymbol{r}_i)$ are forces exerted on A or B atoms at site $\boldsymbol{r}_i$ due to the hard wall at $z = 0$. In the case of a free surface (in contact with vacuum or air) at $z = 0$, it would seem natural to set $\nu_A(\boldsymbol{r}_i) = \nu_B(\boldsymbol{r}_i) = 0$, but in this case any intrinsic roughness of the interface between the mixture and the 'vapour phase' at $z < 0$ is disregarded. This treatment would hold for solids above their roughening transition temperature T_R [30, 31] (and for fluid mixtures where the fluid–gas interface is always rough, of course) only on length scales distinctly larger than the scale of atomic roughness. A second effect due to the breaking of the translational symmetry of the surface

is that, in general, one must expect that the pairwise interactions ϕ_{AA}, ϕ_{AB}, ϕ_{BB} depend not only on the relative distance $(\boldsymbol{r}_i - \boldsymbol{r}_j)$, but also on $\boldsymbol{r}_i, \boldsymbol{r}_j$ separately (e.g., different interactions occur if both sites i, j are in the layer adjacent to the surface [32, 33].

One is not interested here in the 'correct' description of atomistic detail, but rather figure 3 and the Hamiltonian in equation (5) only serve as a generic model for deriving a reasonable continuum description which holds for a much larger class of systems [32, 34, 35]. We simplify the problem by restricting the range of all interactions to nearest neighbours, and take all interactions $\phi_{AA}, \phi_{AB}, \phi_{BB}$ to be independent of their sites i, j except if both sites are in the surface layer $n = 1$. Finally, we assume $\nu_A(\boldsymbol{r}_i)$, $\nu_B(\boldsymbol{r}_i)$ to be non-zero only if i is in the layer $n = 1$. This latter assumption, however, means that one restricts attention to wetting with short-range forces, and it is well known that this situation differs in important qualitative respects from wetting with long-range forces [35], e.g., van der Waals forces which decay as z^{-3}, where z is the distance from the surface. In recent work, we have also considered the effect of long-ranged surface forces on the dynamics of phase separation and will present some results for this case later.

It is convenient to translate our lattice-gas model into the Ising-spin representation via the usual transformation $c_i = (1 - S_i)/2$ $(S_i = \pm 1)$, which yields

$$\mathcal{H} - \mu_A \sum_i c_i - \mu_B \sum_i (1 - c_i) = -\sum_{\langle i,j \rangle} J_{ij} S_i S_j - H \sum_i S_i - H_1 \sum_{i \in \text{1st layer}} S_i + \mathcal{H}_0 \qquad (6)$$

where μ_A, μ_B are the chemical potentials of both species, and $\mathcal{H}_0$ is a constant which only affects the energy scale. The pairwise 'exchange' interaction J_{ij} is

$$J_{ij} = J = \frac{1}{2}\phi_{AB} - \frac{1}{4}(\phi_{AA} + \phi_{BB}) \qquad (7)$$

when at least one of the sites i, j is not in the surface layer $n = 1$. If both sites are in the layer $n = 1$,

$$J_{ij} = J_s = \frac{1}{2}\phi_{AB}{}^s - \frac{1}{4}(\phi_{AA}{}^s + \phi_{BB}{}^s) \qquad (8)$$

where the superscript s refers to the pairwise interaction potentials in the surface layer. The bulk 'magnetic field' H is (for sites i not in the $n = 1$ layer)

$$H = \frac{1}{2}(\mu_B - \mu_A) + \frac{1}{2}\sum_{j(\neq i)} (\phi_{AA} - \phi_{BB}) \qquad (9)$$

while for sites i in the $n = 1$ layer one has an additional 'surface field' H_1,

$$H + H_1 = \frac{1}{2}(\mu_B - \mu_A + \nu_A - \nu_B) + \frac{1}{2}\left[\sum_{j \in \text{1st layer}\ j(\neq i)} (\phi_{AA}{}^s - \phi_{BB}{}^s) + \sum_{j \in \text{2nd layer}} (\phi_{AA} - \phi_{BB})\right]. \qquad (10)$$

A non-zero surface field H_1 arises even for the case where $\nu_A = \nu_B = 0$ and interactions are unchanged near the surface, i.e., $\phi_{AA}{}^s = \phi_{AA}$ and $\phi_{BB}{}^s = \phi_{BB}$, as long as $\phi_{AA} - \phi_{BB} \neq 0$. This is a result of the 'missing neighbours' of sites in the first layer. Considering the most symmetric case, where $\phi_{AA} = \phi_{BB}$, clearly has little physical relevance for actual mixtures. The 'bulk field' in equation (9) is easily eliminated from the problem by fixing the average concentration

$$\bar{c} = \frac{1}{N}\sum_i \langle c_i \rangle \qquad (11)$$

which is also the concentration c_b in the bulk of this semi-infinite system. Thus, the additional surface field H_1 must remain as a parameter in the problem. As is well known [32, 34, 35], this term is responsible for both surface enrichment and wetting phenomena in mixtures.

Both surface critical phenomena [32, 34, 35] and wetting [35, 36] can be discussed in terms of the singular behaviour of the surface excess free-energy density $f_s(T, H, H_1)$, where T is the temperature. This quantity is conveniently defined on the basis of the free-energy density $f(T, H, H_1)$ of a thin film of thickness D with two equivalent surfaces as follows:

$$f(T, H, H_1) = f_b(T, H) + \frac{2}{D} f_s(T, H, H_1) \qquad D \to \infty \tag{12}$$

where $f_b(T, H)$ is the bulk free-energy density of the system at temperature T and bulk field H. Particularly interesting physical quantities are the response functions, e.g., the surface susceptibility χ_s defined as

$$\chi_s = -\left.\frac{\partial^2 f_s(T, H, H_1)}{\partial H^2}\right|_{T,H_1} = \sum_n (\chi_n - \chi_b) = \int_0^\infty \mathrm{d}z\ [\chi(z) - \chi_b] \tag{13}$$

where the bulk susceptibility is $\chi_b = -\partial^2 f_b(T, H)/\partial H^2|_T$. The surface layer susceptibility is defined as

$$\chi_1 = -\left.\frac{\partial^2 f_s(T, H, H_1)}{\partial H\, \partial H_1}\right|_T = \left.\frac{\partial m_1}{\partial H}\right|_{T,H_1} = \beta \sum_j (\langle S_i S_j\rangle_T - \langle S_i\rangle_T \langle S_j\rangle_T) \tag{14}$$

where $m_1 = \langle S_i\rangle_T$, with i being chosen from the first layer and $\beta = (k_B T)^{-1}$. We can also define a susceptibility with respect to the surface field H_1 as

$$\chi_{11} = -\left.\frac{\partial^2 f_s(T, H, H_1)}{\partial H_1^2}\right|_{T,H} = \left.\frac{\partial m_1}{\partial H_1}\right|_{T,H} = \beta \sum_{j\in 1\text{st layer}} (\langle S_i S_j\rangle_T - \langle S_i\rangle_T \langle S_j\rangle_T). \tag{15}$$

The layer magnetization m_n and the layer susceptibilities χ_n, χ_{nn} are obvious generalizations to the case when a field H_n acts on spins in the nth layer:

$$\chi_n = \left.\frac{\partial m_n}{\partial H}\right|_{T,H_n} = \beta \sum_j (\langle S_i S_j\rangle_T - \langle S_i\rangle_T \langle S_j\rangle_T) \qquad i \in n \tag{16}$$

and

$$\chi_{nn} = \left.\frac{\partial m_n}{\partial H_n}\right|_{T,H} = \beta \sum_{j\in n} (\langle S_i S_j\rangle_T - \langle S_i\rangle_T \langle S_j\rangle_T) \qquad i \in n. \tag{17}$$

Of course, equations (16) and (17) are related to the long-wavelength limits of the corresponding structure factors ($\boldsymbol{k}_\parallel$ is a wave-vector lying in a plane parallel to the surface):

$$S_n(\boldsymbol{k}) = \sum_j \exp[\mathrm{i}\boldsymbol{k}\cdot(\boldsymbol{r}_j - \boldsymbol{r}_i)](\langle S_i S_j\rangle_T - \langle S_i\rangle_T \langle S_j\rangle_T) \qquad i \in n \tag{18}$$

and

$$S_{nn}(\boldsymbol{k}_\parallel) = \sum_{j\in n} \exp[\mathrm{i}\boldsymbol{k}_\parallel\cdot(\boldsymbol{r}_j - \boldsymbol{r}_i)](\langle S_i S_j\rangle_T - \langle S_i\rangle_T \langle S_j\rangle_T) \qquad i \in n. \tag{19}$$

In analogy with equation (12), it is reasonable to consider the surface excess $S_s(\boldsymbol{k})$ of the total scattering intensity $S(\boldsymbol{k})$ of a film,

$$S(\boldsymbol{k}) = S_b(\boldsymbol{k}) + \frac{2}{D} S_s(\boldsymbol{k}) \qquad D \to \infty \tag{20}$$

where

$$S_s(\boldsymbol{k}) = \sum_n [S_n(\boldsymbol{k}) - S_b(\boldsymbol{k})] = \int_0^\infty \mathrm{d}z\ [S(\boldsymbol{k}, z) - S_b(\boldsymbol{k})]. \tag{21}$$

In static equilibrium, the small-k behaviour of the structure factors defined via equations (18)–(21) characterizes the typical length scales of the problem: for surface critical phenomena, it is simply the correlation length ξ_b which controls these length scales for both the ordinary and special surface transition [32, 34]. However, for critical wetting, separate correlation lengths $\xi_\parallel, \xi_\perp$ in directions parallel and perpendicular to the surface need to be distinguished [35].

3.2.2. The coarse-grained equivalent of the semi-infinite Ising model with Kawasaki spin-exchange kinetics. The Ising model has no intrinsic dynamics and phase separation in the Ising model is usually mimicked via stochastic Kawasaki spin-exchange kinetics, which allows for the interchange of spins on neighbouring sites. We do the same for the semi-infinite Ising model and use the master equation approach to write down evolution equations for the expectation value of the site spin variable or 'magnetization' [23–25]. Though exact, these equations are not particularly useful as they are analytically and numerically intractable. To proceed further, we invoke the mean-field approximation to obtain closed-form equations for the evolution of the order parameter, i.e., the expectation value of the spin variable. Finally, we coarse grain these equations to obtain the relevant partial differential equation model. We do not wish to replicate this procedure here as it has already been extensively discussed in the literature [23–25]. However, we do caution the reader that the approximations involved are valid only close to the critical point whereas we typically use these models to study phase-ordering dynamics far from criticality. Therefore, we would like to interpret the master equation approach as a guide to good phenomenology rather than as a derivation. Of course, as with all good phenomenology, the resultant model can only be justified by its ability to replicate experimental results.

Having clarified the basis of the master equation approach to these problems, we present the resultant dimensionless model for phase-separation kinetics in the presence of a surface with a delta-function surface potential [25]. As expected, the bulk dynamics is described by the usual CH equation, which is the deterministic version of equation (2). The surface is mimicked by the boundary conditions

$$\begin{aligned} \frac{\partial \phi(\boldsymbol{R}, 0, \tau)}{\partial \tau} &= h_1 + g\phi(\boldsymbol{R}, 0, \tau) + \gamma \left.\frac{\partial \phi(\boldsymbol{R}, Z, \tau)}{\partial Z}\right|_{Z=0} \\ 0 &= \frac{\partial}{\partial Z}\left[\phi(\boldsymbol{R}, Z, \tau) - \phi(\boldsymbol{R}, Z, \tau)^3 + \frac{1}{2}\nabla^2\phi(\boldsymbol{R}, Z, \tau)\right]\Bigg|_{Z=0}. \end{aligned} \tag{22}$$

The first of these boundary conditions rapidly pins the surface value of the order parameter to an equilibrium value dictated by the competition between the surface field and the energy cost associated with a gradient in the order parameter. The second boundary condition is simply the no-flux condition, which we had presented earlier also, and enforces conservation of the order parameter. All variables have been rescaled into dimensionless units and the

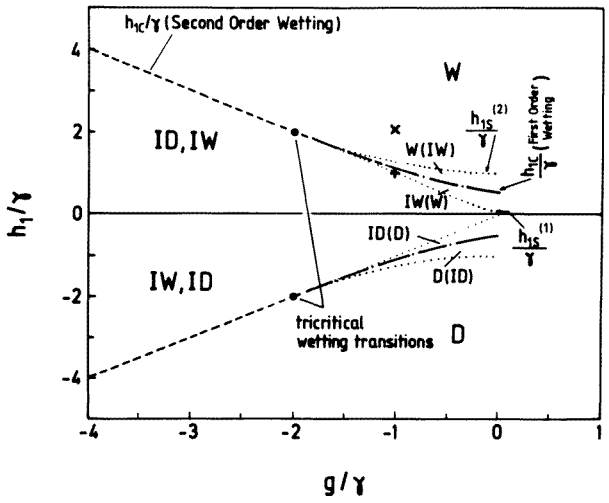

Figure 4. The phase diagram of our dimensionless model for surface-directed spinodal decomposition, obtained by finding the solution of equations (25) and (26). The parameters varied are h_1/γ and g/γ; and the states are labelled as wet (W), incompletely wet (IW), dry (D), and incompletely dry (ID). The phase diagram is symmetric about the axis $h_1/\gamma = 0$. For further details and equations of different lines, see Puri and Binder [25]. Subsequently, we present results for the parameter values $h_1 = 8$, $g = -4$ and $\gamma = 4$, marked by an $\times$ in the phase diagram. (From reference [28].)

parameters in equation (22) are defined in terms of the unscaled parameters as follows:

$$\begin{aligned} h_1 &= \frac{4H_1}{\sqrt{3}T}\left(\frac{T}{T_c}\right)^{3/2}(2q)^{3/2}{\xi_b}^5 \\ g &= 8\left[(q-2)\frac{J_s}{J} - (q-1)\right]{\xi_b}^4 \\ \gamma &= 4{\xi_b}^3. \end{aligned} \tag{23}$$

In equation (23), T_c is the mean-field critical temperature, i.e., $T_c = qJ$, where q is the coordination number of a site. Furthermore, ξ_b $(=[2q(1 - T/T_c)]^{-1/2})$ denotes the bulk correlation length.

In view of the approximations made in obtaining our dynamical model, it is gratifying that the same equations are derivable near criticality solely from symmetry principles, as was demonstrated by Diehl and Janssen [37].

Before discussing the numerical solutions of this semi-infinite non-linear problem or the analytic solutions of the linearized problem, we would like to relate the static surface properties of semi-infinite mixtures to the equilibrium wetting phase diagram and also discuss the general framework for characterization of surface-directed spinodal decomposition.

The static properties of our model described by the CH equation with the boundary conditions in equation (22) can be understood in terms of a free-energy functional [32, 34–36]:

$$\beta\mathcal{F} = \int \mathrm{d}\boldsymbol{R}\left[\left\{\int_0^\infty \mathrm{d}Z\left(\frac{1}{4}(\boldsymbol{\nabla}\phi)^2 - \frac{1}{2}\phi^2 + \frac{1}{4}\phi^4\right)\right\} - \frac{1}{2}\frac{h_1}{\gamma}\phi_1 - \frac{1}{4}\frac{g}{\gamma}{\phi_1}^2\right] \tag{24}$$

where $\phi_1(\boldsymbol{R}) \equiv \phi(\boldsymbol{R}, Z = 0)$ is the local order parameter at the surface, and we consider the critical region where $T \simeq T_c$.

The surface phase diagram that results from the free energy in equation (24) has been discussed in previous work [27, 28]. Figure 4 shows the phase boundaries in the plane of the variables h_1/γ and g/γ. These phase boundaries result from minimizing the free-energy functional in equation (24), which yields the Euler–Lagrange equation ($\phi(\boldsymbol{R}, Z)$ can be taken as being independent of $\boldsymbol{R}$):

$$\phi(Z) - \phi(Z)^3 + \frac{1}{2}\frac{\mathrm{d}^2\phi(Z)}{\mathrm{d}Z^2} = 0 \tag{25}$$

with the boundary condition

$$\frac{h_1}{\gamma} + \frac{g}{\gamma}\phi(0) + \left.\frac{\mathrm{d}\phi(Z)}{\mathrm{d}Z}\right|_{Z=0} = 0. \tag{26}$$

Equations (25) and (26) are compatible with the static limit of (the deterministic version of) equation (2) and equation (22), as would be expected. Note that, for unchanged interactions at the surface ($J_s = J$), and near criticality ($\xi_b \to \infty$), one has $g/\gamma = -2\xi_b \to -\infty$, $h_1/\gamma \propto H_1{\xi_b}^2 \to \infty$, i.e., one is typically in the region where the surface is wet far above the second-order wetting transition on the left-hand side of the phase diagram (for $h_1 > 0$). However, since in a typical experimental situation one is interested in spinodal decomposition and wetting far from the bulk critical point, we shall use the present model for parameter choices of g, h_1, γ of order unity as well.

The phenomenology in equilibrium discussed earlier readily provides the appropriate theoretical framework for defining quantities which are needed to characterize surface effects on spinodal decomposition. In the non-equilibrium case, one again considers equal-time correlation functions and structure factors of the type defined in equations (18)–(21), which are now time dependent since one considers quenching experiments far from thermal equilibrium. Thus, the quantities that we wish to consider are the order parameter correlation function

$$G_{\parallel}(\boldsymbol{R}_1 - \boldsymbol{R}_2, Z, \tau) = \langle\phi(\boldsymbol{R}_1, Z, \tau)\phi(\boldsymbol{R}_2, Z, \tau)\rangle - \langle\phi(\boldsymbol{R}_1, Z, \tau)\rangle\langle\phi(\boldsymbol{R}_2, Z, \tau)\rangle \tag{27}$$

where $\phi(\boldsymbol{R}, Z, \tau)$ is the continuum time-dependent order parameter in dimensionless units, or its Fourier transform

$$S_{\parallel}(\boldsymbol{k}_{\parallel}, Z, \tau) = \int \mathrm{d}\boldsymbol{R}\ \exp(\mathrm{i}\boldsymbol{k}_{\parallel}\cdot\boldsymbol{R})G_{\parallel}(\boldsymbol{R}, Z, \tau). \tag{28}$$

In equation (27), the angular brackets denote averages over both initial conditions and thermal noise. We can also consider the more general correlation function

$$G(\boldsymbol{R}_1 - \boldsymbol{R}_2, Z_1, Z_2, \tau) = \langle\phi(\boldsymbol{R}_1, Z_1, \tau)\phi(\boldsymbol{R}_2, Z_2, \tau)\rangle - \langle\phi(\boldsymbol{R}_1, Z_1, \tau)\rangle\langle\phi(\boldsymbol{R}_2, Z_2, \tau)\rangle \tag{29}$$

and its counterpart in Fourier space (accounting for the breaking of translational symmetry by the wall)

$$S(\boldsymbol{k}, Z, \tau) = \int \mathrm{d}\boldsymbol{R}\ \int_0^\infty \mathrm{d}Z'\ \exp(\mathrm{i}\boldsymbol{k}_{\parallel}\cdot\boldsymbol{R} + k_{\perp}(Z' - Z))G(\boldsymbol{R}, Z', Z, \tau). \tag{30}$$

In both equations (28) and (30), we have made use of the translational invariance in the direction parallel to the surface. Note that, in our definition, $G_{\parallel}(\boldsymbol{R}_1 - \boldsymbol{R}_2, Z, \tau) =$

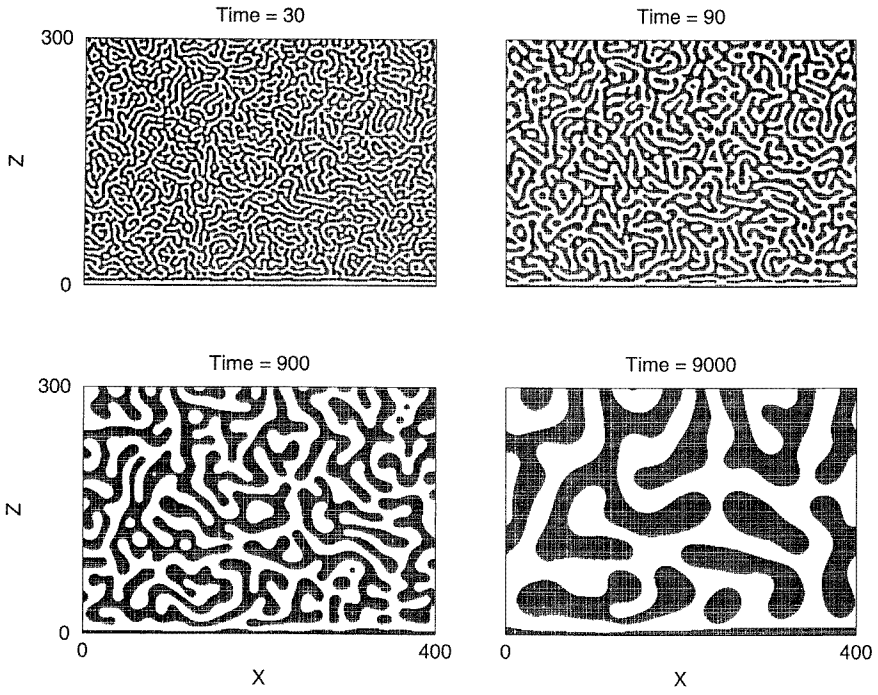

Figure 5. Evolution pictures from an Euler-discretized version of our dynamical model consisting of the CH equation in conjunction with the boundary conditions in equation (22). The parameter values were $h_1 = 8$, $g = -4$ and $\gamma = 4$, corresponding to a wet static equilibrium, marked by an $\times$ in the phase diagram of figure 4. Our two-dimensional results were obtained on a lattice of size $L_X \times L_Z$ ($L_X = 400$ and $L_Z = 300$, in this case) with discretization mesh sizes $\Delta\tau = 0.03$ and $\Delta X = 1.0$. The surface with a delta-function potential is located at $Z = 0$ and is mimicked by the boundary conditions in equation (22). Free boundary conditions are applied at $Z = L_Z$ and periodic conditions are applied in the X-direction. The initial condition consists of uniformly distributed random small-amplitude fluctuations about a zero background, mimicking the disordered state before the quench. Evolution pictures are shown for the dimensionless times $\tau = 30, 90, 900$ and 9000.

$G(\boldsymbol{R}_1 - \boldsymbol{R}_2, Z, Z, \tau)$. In analogy with equation (21), the surface excess of the time-dependent scattering intensity of the system is then

$$S_s(\boldsymbol{k}, \tau) = \int_0^\infty \mathrm{d}Z \; [S(\boldsymbol{k}, Z, \tau) - S_b(\boldsymbol{k}, \tau)] \tag{31}$$

where $S_b(\boldsymbol{k}, \tau)$ is the scattering intensity observed in the bulk.

In studies of spinodal decomposition, one usually defines length scales from the decay of the real-space correlation function or by taking reduced moments of the momentum-space structure factor. We define the characteristic length $L_\parallel(Z, \tau)$ describing the growth of correlations in the parallel direction at a distance Z from the surface as the distance over which the appropriate real-space correlation function decays to half its maximum value. Thus, in two-dimensional space,

$$G_\parallel(L_\parallel(Z, \tau), Z, \tau) = G_\parallel(0, Z, \tau)/2. \tag{32}$$

This definition proved easy to implement in the context of our numerical calculations and was thus used in all of our simulations. Of course, a perpendicular length scale $L_\perp(Z, \tau)$

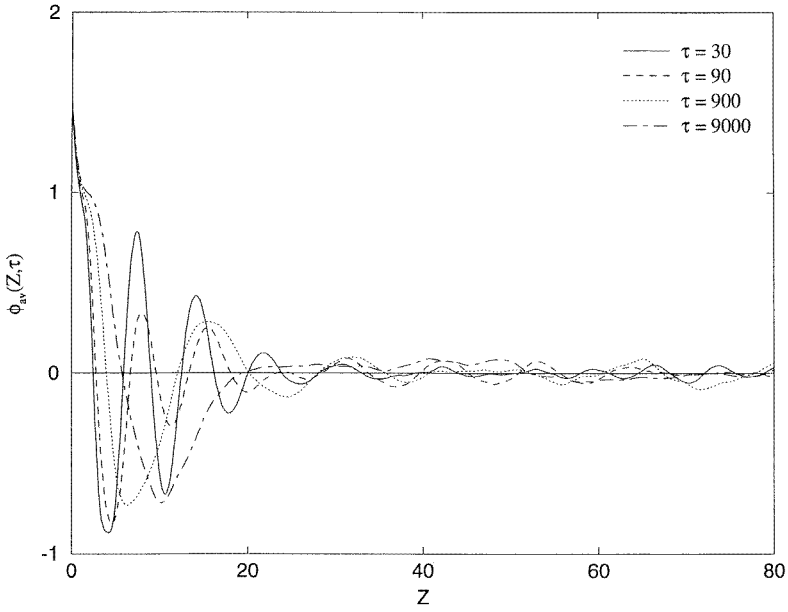

Figure 6. Laterally averaged order parameter profiles $\phi_{\rm av}(Z,\tau)$ versus Z for the evolution depicted in figure 5. These profiles are obtained as an average over 200 independent runs, with the order parameter being further averaged in the X-direction for each separate run.

can be defined similarly. For $Z \to \infty$, these scales $L_{\parallel}(Z,\tau)$ and $L_{\perp}(Z,\tau)$ should tend smoothly towards the length scales that one uses to characterize spinodal decomposition in the bulk, which we denote simply as $L_b(\tau)$.

3.2.3. Numerical results for surface-directed spinodal decomposition. We have performed extensive numerical simulations of our model consisting of the CH equation supplemented by the boundary conditions in equation (22). These simulations were conducted using a simple Euler discretization scheme on two-dimensional lattices of size $L_X \times L_Z$ [25, 29]. The discretization mesh sizes for the results presented here are $\Delta\tau = 0.03$ and $\Delta x = 1.0$, except where stated otherwise. The surface was taken to be located at $Z = 0$ and this was modelled using the boundary conditions in equation (22). Free boundary conditions were applied at $Z = L_Z$ and periodic boundary conditions were applied in the X-direction. Details of our simulation and extensive results are provided in references [25] and [29] and we will only present representative results here. We should stress that our simulations are deterministic and correspond to the low-noise limit. Our primary interest in these simulations was to investigate the interplay between the wetting layer at the wall and spinodal decomposition in the bulk. When the surface field is weak compared to the thermal noise, the surface is only partially wetted and domains of both phases are in contact with the wall. We shall discuss this situation in the next subsection.

Figure 5 shows typical evolution pictures for a set of parameter values ($h_1 = 8, g = -4, \gamma = 4$), where the surface is completely wetted by the preferred phase in equilibrium. The corresponding point is marked by an $\times$ in the phase diagram of figure 4. The initial condition for figure 5 is a uniformly disordered state corresponding to a high temperature. At

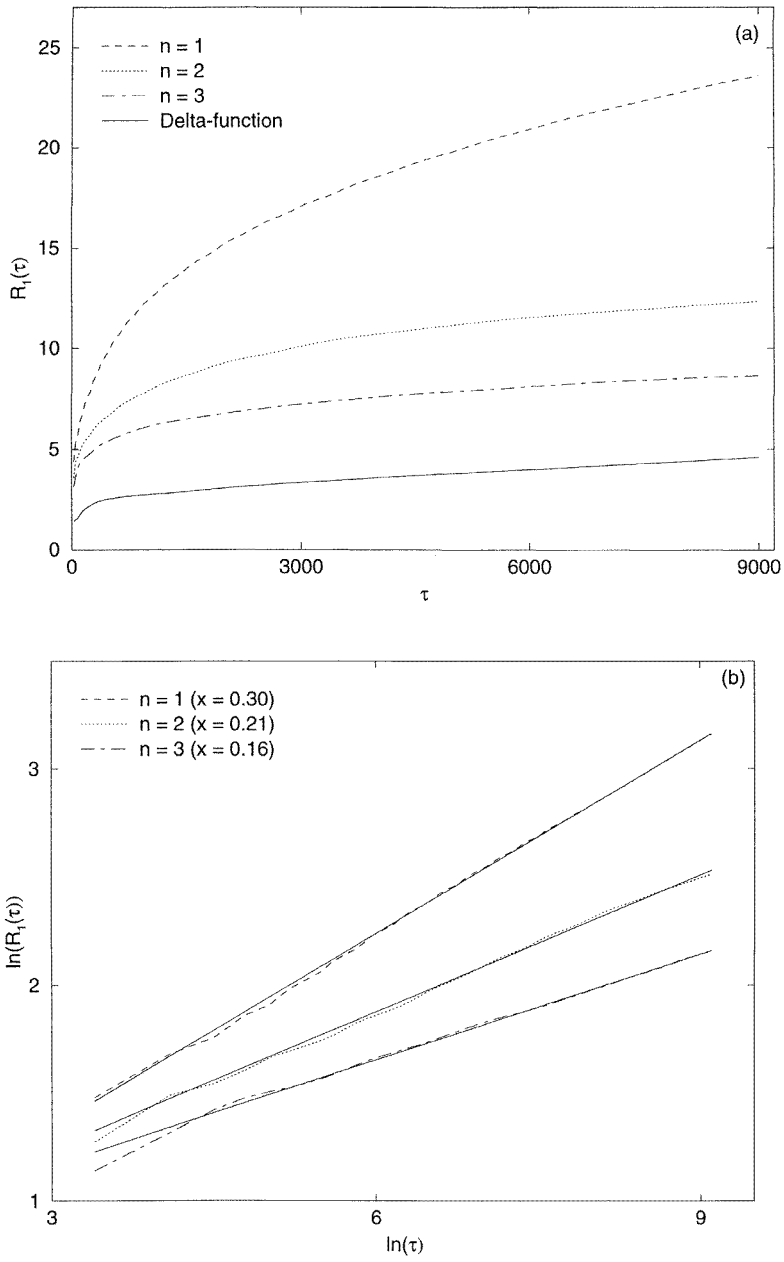

Figure 7. (a) The position of the first zero of the laterally averaged order parameter profiles $R_1(\tau)$ versus τ for the cases of a surface with a delta-function potential, and a long-ranged $1/Z^n$ potential with $n = 1, 2$ and 3 [29]. (b) A log–log plot of data for the cases with the long-ranged potential in figure 7(a). The solid lines denote the best linear fits to the different data sets. The best-fit exponents are $x = 0.30, 0.21$ and 0.16 for $n = 1, 2$ and 3, respectively. The error bars for these exponent values are ± 0.01.

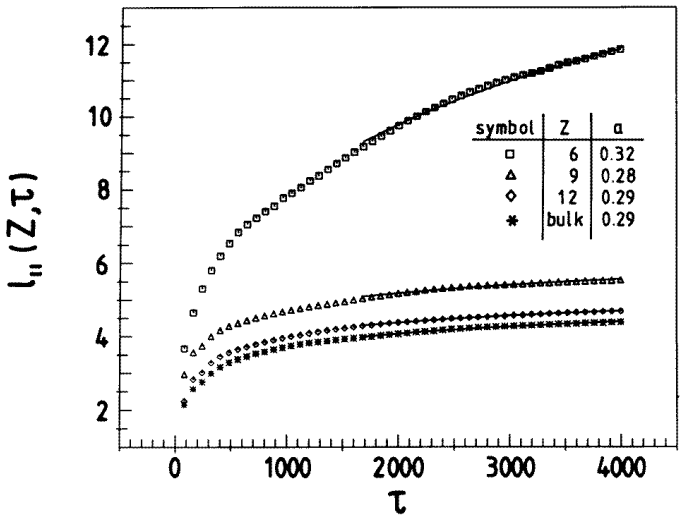

Figure 8. Layer-dependent length scales in the direction parallel to the surface $L_{\parallel}(Z, \tau)$ versus τ for surface-directed spinodal decomposition with a delta-function surface potential. The parameter values are $h_1 = 8, g = -4$ and $\gamma = 4$, as in figure 5. These length scales are defined as the distance over which the corresponding layerwise correlation function decays to half its maximum value. The correlation function data is obtained on lattices of size $L_X \times L_Z$ ($L_X = 300, L_Z = 150$) with discretization mesh sizes $\Delta\tau = 0.05$ and $\Delta X = 1.5$, as an average over 20 independent runs. We present data for $Z = 6, 9, 12$ and the bulk case, denoted by the symbols indicated. The solid lines superposed on the data sets correspond to non-linear best fits to the functional form $a + b\tau^a$ for $\tau > 1600$ and the best-fit exponents (with error bars ± 0.02) are indicated on the figure. (From reference [25].)

the dimensionless time $\tau = 0$, the system is quenched below the bulk critical temperature and allowed to evolve deterministically. The surface forms a layer rich in the preferred phase followed by a layer rich in the other phase, while the bulk shows the usual isotropic spinodal decomposition. The enriched layers at the surface coarsen with time. Figure 6 shows laterally averaged order parameter profiles $\phi_{\text{av}}(Z, \tau)$ as a function of the distance from the surface Z and is the numerical equivalent of figures 1 and 2(a). The surface region shows the damped oscillatory profile also seen in figures 1 and 2(a) and these surface-directed waves propagate into the bulk with the passage of time. In the bulk, of course, lateral averaging over randomly directed wave-vectors gives a near-zero value for the order parameter.

One of the most interesting and experimentally relevant quantities is the time dependence of the first zero of these laterally averaged profiles. Figure 7 plots the position of the first zero $R_1(\tau)$ versus τ for the case with a delta-function surface potential, which we have been considering so far, and also for cases with a long-ranged surface potential $V(Z) \sim 1/Z^n$ with $n = 1$, 2 and 3 [29]. Of course, at the surface we have to flatten out the potential and we choose a situation in which the surface field is also $h_1 = 8$ [29]. Figure 7(a) is a direct plot of $R_1(\tau)$ versus τ for the delta-function case and the long-ranged cases with $n = 1, 2, 3$, and figure 7(b) is a log–log plot of the data for $n = 1, 2, 3$. The growth of the surface layer is very slow in the delta-function case and is possibly logarithmic, though we do not have sufficiently extended data to conclusively confirm this. The data for the long-ranged cases appear to obey a reasonable power law over the time-scales considered,

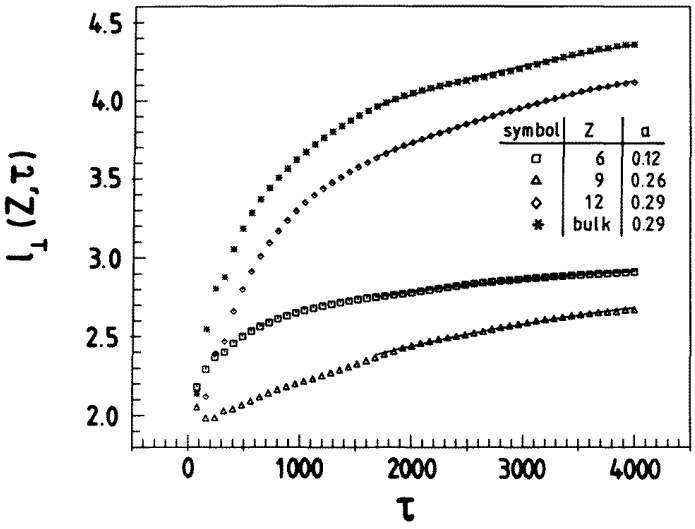

Figure 9. The time dependence of layerwise length scales in the direction perpendicular to the surface, denoted by $L_\perp(Z,\tau)$. Data sets correspond to the same values of Z as in figure 8; and the superposed solid lines denote non-linear best fits to the functional form $a + b\tau^a$ for $\tau > 1600$. The corresponding best-fit exponents are marked on the figure and are consistent with Lifshitz–Slyozov growth except in the immediate vicinity of the surface at $Z = 6$. (From reference [25].)

but the best-fit exponent (denoted by x in figure 7(b)) depends on the nature of the potential. These results should be contrasted with those for the limit of low field and high noise, where the surface layer thickness always exhibits a LS growth law.

The extremely slow growth of the wetting layer in the case with a delta-function potential has an important implication for surface-directed spinodal decomposition, namely, the dynamics of the wetting layer does not actively interfere with the dynamics of phase separation. However, the presence of a wetting layer at the surface provides a preferred direction of alignment for domains near the surface. Thus, growth parallel to the surface is faster nearer the surface than in the bulk. This is shown in figure 8, where we plot $L_\parallel(Z,\tau)$ versus τ for different values of Z. However, the data for $L_\parallel(Z,\tau)$ are always consistent with the LS growth law $L_\parallel(\tau) = a + b\tau^{1/3}$ and the enhanced growth near the surface is a result of larger coefficients a and b rather than a different growth exponent. Figure 9 shows the time dependence of the Z-dependent length scale perpendicular to the surface, denoted by $L_\perp(Z,\tau)$. Apart from the data for $Z = 6$, other growth exponents again appear to be consistent with the LS growth law. We interpret the small effective exponent near the surface as a weighted average of the growth exponent of the wetting layer and the LS exponent $\phi = 1/3$ which applies in the bulk. This picture appears to be consistent with the recent experiments by Geoghegan *et al* [13], which we had mentioned in the previous section.

We have also investigated the experimentally relevant problem of spinodal decomposition in a thin-film geometry [38]. The walls of the thin film are mimicked by two sets of boundary conditions of the type in equation (22). For details of our simulation and results, we refer the interested reader to reference [38].

3.3. Other relevant studies

In this subsection, we would like to discuss a number of other important studies of this problem. Brown and Chakrabarti [9] presented results from a two-dimensional simulation of surface-directed spinodal decomposition with both short-ranged and long-ranged surface fields. They modelled 'bulk' phase separation by the CHC equation with a surface potential term. The surface was mimicked by two boundary conditions—one fixing the order parameter at the surface to its value in the preferred phase, and the other one corresponding to the usual no-flux condition. The parameter values used by these authors correspond to the low-field–high-noise regime. Brown and Chakrabarti found that the thickness of the enriched surface layer in their simulation obeys the LS growth law $R_1(\tau) \sim \tau^{1/3}$. Furthermore, they showed that length scales perpendicular and parallel to the surface are also consistent with a LS growth law, but the typical domain sizes parallel to the surface are larger than those perpendicular to the surface—in conformity with our results from the previous section. Finally, Brown and Chakrabarti found that the time-dependent surface-directed wave profiles had a simple scaling form, namely, $\phi_{\rm av}(Z,\tau) = \Phi(Z/R_1(\tau))$. This should be contrasted with the high-field–low-noise limit, where the morphology of the laterally averaged profiles also evolves in time and the simple scaling *ansatz* proposed above does not apply. Bhattacharya *et al* [39] have used a similar model to study spinodal decomposition in a strip geometry. Recently, Brown *et al* [40] have also reported an interesting study of 'surface-induced nucleation', where they consider a metastable binary mixture in contact with a surface which can nucleate droplets of the preferred phase with much greater facility than in the bulk. In this situation, they find that the thickness of the 'wetting layer' exhibits a crossover from the LS growth law ($R_1(\tau) \sim \tau^{1/3}$) to a slower growth law ($R_1(\tau) \sim \tau^{1/6}$). We believe that a more detailed experimental and numerical investigation of the nucleation regime would be of considerable interest.

Brown and Chakrabarti have also used similar models to investigate surface-directed spinodal decomposition in block copolymer melts in both semi-infinite and strip geometries [41]. Following Oono and Shiwa [42], they modelled the block copolymer system via the usual ϕ^4-free-energy functional in conjunction with a long-ranged interaction term. The boundary conditions, which mimicked the surface, were the same as in their previous study. As expected, the additional long-ranged interaction term in the free-energy functional drastically modifies the bulk and surface dynamics of the phase-separating system. For details of this study, we refer the interested reader to reference [41].

A comprehensive cell dynamical system (CDS) study of this problem was reported by Marko [10]. He also considered surface-directed spinodal decomposition with both short-ranged and long-ranged surface forces. In our perception, Marko's study is one of the most thorough investigations of this problem. He considered both two- and three-dimensional systems, and also studied both the low-surface-field–high-noise and high-surface-field–low-noise limits. Marko carefully clarified the morphologies of domain growth and the laterally averaged profiles in both limits, though his primary focus was the limit in which the surface is only partially wet. In this limit, he found results consistent with those of Brown and Chakrabarti [9] for the growth of wetting layers. On the other hand, in the low-noise limit, he found a drastic slowing down of the growth of the wetting layer into the bulk, in conformity with our results. However, he did not attempt to quantify the nature of domain growth laws in the low-noise limit. Marko also presented an analysis of the effect of hydrodynamic flows on surface structure in the asymptotic time regime.

Another important study is due to Ma *et al* [43], who approached this problem via two different simulations. The first of these was a molecular dynamics (MD) study of a binary

Lennard-Jones fluid mixture phase separating in the presence of a wall. Their MD study showed surface-directed spinodal decomposition waves analogous to the study of Jones *et al* [6], and the numerical results that we have shown earlier. Ma *et al* defined length scales through moments of the time-dependent structure factor of the composition profiles. However, they were unable to make clear quantitative statements about the behaviour of these characteristic length scales. The second simulation reported by Ma *et al* [43] was a study of a system of Langevin equations for soft-spin variables on a discrete spatial lattice. Again, they observed waves of surface-directed spinodal decomposition, as in their MD study. The domain growth in this case appears to be somewhat slower than in their MD study but the difference needs to be quantified more clearly.

Finally, we mention a MC study by Sagui *et al* [44], who investigated surface-directed phase separation in three dimensions. These authors considered an Ising model with a short-ranged surface field and Kawasaki spin-exchange kinetics. They studied situations with both zero and non-zero surface fields. In the absence of a surface field, phase separation can occur in the surface layer by an appropriate adjustment of the interactions in the surface and bulk layers, even if the bulk is stable. For the case of a stable bulk and unstable surface, Sagui *et al* reported that the lateral domain growth in the surface layer was consistent with the LCA growth law, namely, $L_{\parallel}(\tau) = a + b\tau^{1/2}$, which characterizes bulk domain growth in the case with non-conserved order parameter. For the case where both the bulk and surface are unstable, Sagui *et al* found that the growth exponent in the surface layer ranged from $\phi = 1/2$ to $\phi = 1/3$, depending on the depth of the quench—with a lower growth exponent for deeper quenches. Nevertheless, in both cases above, Sagui *et al* found that the scaled structure factor in the surface layer is consistent with the Ohta–Jasnow–Kawasaki form [45], which characterizes domain growth in the non-conserved case. Sagui *et al* also considered the case with non-zero surface field, where they observed similar behaviour. Their results should be contrasted with the numerical and experimental results cited earlier, which found that the lateral length scale in the surface layer also obeys the LS growth law.

3.4. Analytical approaches to early-time (linear) behaviour

The non-linear model discussed in subsection 3.2 (i.e., the CH equation in conjunction with the boundary conditions in equation (22)) is clearly not amenable to analytic solution, except in the static limit. However, one can solve the linearized version of this model and thereby obtain useful information in certain relevant limits. In the bulk, solution of the linearized model is rather trivial. In the present case, however, one has to account for the two boundary conditions at the surface and this makes the problem considerably more difficult.

Binder and Frisch [24] first solved the linearized problem for the case of a stable bulk ($T > T_c$). They studied the approach to equilibrium of a homogeneous initial condition and showed that the resultant concentration profile has a transient minimum whose distance from the wall grows as $\tau^{1/2}$. Qualitatively, these concentration profiles strongly resemble those reported by Jones and Kramer [46] in their experimental studies of surface enrichment in binary polymer mixtures. At later times, the concentration profile obtained from the linear theory exhibits an essentially exponential decay with the equilibrium correlation length. For long times, the order parameter profile can be approximated as the sum of two exponentially decaying terms. One of the relaxation times, related to the equilibrium correlation length, is effectively constant and the other one, reflecting the diffusive behaviour, is proportional to $\tau^{1/2}$. This results in a diffusive behaviour of the spatial moments, in which the nth moment of the profile diverges as $\tau^{n/2}$. These results were confirmed numerically by Puri

and Frisch [47], who also demonstrated that the broad features of the surface-enrichment profile exhibited a diffusive behaviour even for strong surface fields, where the linearized theory was not valid.

Frisch *et al* [48] also examined surface-directed spinodal decomposition in the framework of a linearized theory. They found that the initial-stage behaviour already replicated reasonably well the damped concentration profiles seen in figures 1 and 6. Furthermore, the predicted wavelength of the concentration oscillations was also compatible with numerical results obtained from the fully non-linear model [25].

4. Summary and discussion

We would like to end this article with a brief summary and discussion of the material presented in this paper. We have attempted to provide a critical overview of the modelling and simulation of surface-directed spinodal decomposition. To motivate the theoretical modelling, we have also provided a brief perspective of experimental results which must be captured by any reasonable model. (For further details of the experimental techniques and results in this area, we refer the interested reader to reference [5].) We do not claim that the present article constitutes an exhaustive review of the theoretical and numerical work in this field. Rather, we have extensively discussed our own contributions to this problem and have highlighted many other important works in the context of our own work.

Before we proceed, it is worthwhile contrasting different levels of modelling of this problem. The simplest level of modelling is the microscopic level, i.e., that via Monte Carlo (MC) or molecular dynamics (MD) simulations of a semi-infinite Ising model with Kawasaki spin-exchange kinetics [21, 43, 44]. Unfortunately, because of their inherent limitations, MC simulations have not had much success in accessing the late stages of spinodal decomposition in the bulk. Thus, it is reasonable to assume that the more complicated problem of surface-directed spinodal decomposition will prove even harder to investigate using MC simulations. On the other hand, coarse-grained models have been very successful in investigating the asymptotic behaviour of bulk spinodal decomposition [49] and this appears to be a reasonable approach to the study of surface-directed spinodal decomposition also.

Successful phenomenological models of surface-directed spinodal decomposition typically consist of a bulk equation which describes phase separation, namely, the CHC equation, in conjunction with two boundary conditions which model the wall. (One can also model spinodal decomposition in a thin-film geometry by applying a pair of appropriate boundary conditions at each wall of the film.) If the surface exerts a long-ranged force on the preferred component, the bulk CHC equation must explicitly incorporate this term. In the case of a delta-function potential at the surface, the surface field is only manifested in the boundary conditions. The first of the two boundary conditions rapidly pins the order parameter at the surface to its equilibrium value, dictated by the competition between the surface field and the order parameter gradient. The second boundary condition is the no-flux condition, which enforces conservation of the order parameter.

We have obtained a phenomenological model by applying the master equation approach to the appropriate microscopic model [24, 25]. Other authors [19, 7, 9, 10] have obtained similar models by the more heuristic method of incorporating suitable surface energy terms into the Ginzburg–Landau free energy. We believe that all these models are in the same dynamical universality class, except those of references [19] and [7], of course. Nevertheless, we feel that the master equation approach that we use has certain advantages over the heuristic method. The first advantage is that it provides a somewhat mechanistic

(and therefore infallible!) method for obtaining a reasonable phenomenological model from an appropriate microscopic model, which is usually easy to formulate. The second advantage is that the incorporation of microscopic detail provides a more accurate modelling of the range of static solutions for the model.

The non-linear phenomenological models thus obtained can only be solved numerically. There are two distinct limits which are of interest. The first possibility is that of strong thermal noise and weak surface field [9, 10]. In this case, domains of both phases are in contact with the surface, so it is only partially wet. In this situation, a strong universality applies in that both the first zero of the laterally averaged order parameter profiles and the lateral domain size obey the Lifshitz–Slyozov growth law. The experiments of references [8, 11] are in accordance with these numerical results. We have studied the opposite limit of strong surface field and no noise as we were primarily interested in the interplay of wetting and spinodal decomposition. In this limit, the surface is completely covered by a layer of the preferred phase and the growth of this layer is governed by the nature of the interaction exerted by the surface on the system. In the case of a delta-function potential at the surface, the wetting layer grows extremely slowly (possibly logarithmically) and does not actively interfere with spinodal decomposition in the bulk. However, the multilayered structure at the surface provides a preferred orientation for domains in the vicinity of the surface. Thus, the growth parallel to the surface is faster than that perpendicular to the surface, though growth laws in both directions appear to the compatible with the LS growth law. We have also studied the functional form of the layer-dependent correlation function parallel to the surface and refer the interested reader to reference [25]. Furthermore, we have also numerically investigated the case with long-ranged surface fields and will present detailed results in reference [29]. The experiments of Geoghegan *et al* [13] appear to realize the high-surface-field–low-noise limit, as do experiments on binary fluids in contact with a surface.

There are a number of important problems which still need to be addressed in this field. For example, there does not appear to be any comprehensive study of off-critical binary mixtures phase separating near a surface, though there has been a preliminary study of surface-induced nucleation [40]. In the absence of hydrodynamic effects, this study should be easy to perform in the framework of the present model. It would also be of great experimental relevance to systematically examine the effects of increasing off-criticality on the morphology of surface-directed spinodal decomposition. An even more important outstanding problem is the incorporation of hydrodynamic effects into the modelling and simulations of this problem. Binary fluids in contact with surfaces are of great experimental and technological relevance [14, 17, 18]. Hydrodynamic effects play a crucial role in the late stages of phase separation in binary fluids [3, 4] and drastically alter the asymptotic domain growth law. A reasonable phenomenological model of phase-separating binary fluids is the so-called model H, which couples dynamical equations for the order parameter and fluid velocity fields [26]. An appropriate phenomenological model for binary fluids phase separating near a surface would consist of model H in the bulk, in conjunction with boundary conditions on both the order parameter and velocity fields. The boundary conditions in equation (22) should be reasonable for binary fluids also, as the fluid velocity is zero at the surface. The obvious boundary condition for the velocity field is to set it to zero at the wall. Though the model is reasonably easy to set up, simulations will be rather demanding because of the large system sizes needed to model hydrodynamic systems so as to avoid finite-size effects [4]. However, these should certainly be within the scope of present-day computing facilities.

Acknowledgments

The authors are extremely grateful to K Binder for a close collaboration on some of the problems described in this article. They are also grateful to him for suggesting that they write this article and for a careful and critical reading of this manuscript. SP would also like to thank R Bausch, A J Bray, R A L Jones, G Krausch and J Marko for useful discussions and comments. In particular, he is grateful to R A L Jones and G Krausch for permission to reproduce their original figures. Finally, SP would like to thank K Binder for his kind hospitality in Mainz during the period in which this paper was completed. His stay in Mainz was supported by the Deutsche Forschungsgemeinschaft (DFG) under Sonderforschungsbereich 262. HLF is grateful to the Humboldt Foundation for the award of a Humboldt prize, which supported his stay in Mainz. He was also supported, in part, by NSF Grant DMR 962-8224.

References

[1] For reviews, see
Gunton J D, San Miguel M and Sahni P S 1983 *Phase Transitions and Critical Phenomena* vol 8, ed C Domb and J L Lebowitz (New York: Academic) p 267
Binder K 1991 *Phase Transformations of Materials (Materials Science and Technology 5)* ed R W Cahn, P Haasen and E J Kramer (Weinheim: VCH) p 405
Bray A J 1994 *Adv. Phys.* **43** 357
[2] Binder K and Stauffer D 1974 *Phys. Rev. Lett.* **33** 1006
Binder K and Stauffer D 1976 *Z. Phys.* B **24** 406
[3] Siggia E D 1979 *Phys. Rev.* A **20** 595
[4] Koga T and Kawasaki K 1991 *Phys. Rev.* A **44** R817
Puri S and Dunweg B 1992 *Phys. Rev.* A **45** R6977
Shinozaki A and Oono Y 1993 *Phys. Rev.* E **48** 2622
Bastea S and Lebowitz J L 1995 *Phys. Rev.* E **52** 3821
[5] Krausch G 1995 *Mater. Sci. Eng. Rep.* R **14** 1
[6] Jones R A L, Norton L J, Kramer E J, Bates F S and Wiltzius P 1991 *Phys. Rev. Lett.* **66** 1326
[7] Ball R C and Essery R L H 1990 *J. Phys.: Condens. Matter* **2** 10 303
[8] Krausch G, Dai C-A, Kramer E J and Bates F S 1993 *Phys. Rev. Lett.* **71** 3669
[9] Brown G and Chakrabarti A 1992 *Phys. Rev.* A **46** 4829
[10] Marko J F 1993 *Phys. Rev.* E **48** 2861
[11] Straub W, Bruder F, Brenn R, Krausch G, Bielefeldt H, Kirsch A, Marti O, Mlynek J L and Marko J F 1995 *Europhys. Lett.* **29** 353
See also
Bruder F and Brenn R 1992 *Phys. Rev. Lett.* **69** 624
[12] Krausch G, Mlynek J, Straub W, Brenn R and Marko J F 1994 *Europhys. Lett.* **28** 323
[13] Geoghegan M, Jones R A L and Clough A S 1995 *J. Chem. Phys.* **103** 2719
[14] Wiltzius P and Cumming A 1991 *Phys. Rev. Lett.* **66** 3000
Cumming A, Wiltzius P, Bates F S and Rosedale J H 1992 *Phys. Rev.* A **45** 885
Harrison C, Rippard W and Cumming A 1995 *Phys. Rev.* E **52** 723
[15] Troian S 1993 *Phys. Rev. Lett.* **71** 1399
Troian S 1994 *Phys. Rev. Lett.* **72** 3739
[16] Keblinski P, Ma W J, Maritan A, Koplik J and Banavar J R 1994 *Phys. Rev. Lett.* **72** 3738
[17] Guenoun P, Beysens D and Robert M 1990 *Phys. Rev. Lett.* **65** 2406
Guenoun P, Beysens D and Robert M 1991 *Physica* A **172** 137
[18] Tanaka H 1993 *Phys. Rev. Lett.* **70** 53
Tanaka H 1993 *Phys. Rev. Lett.* **70** 2770
Tanaka H 1993 *Europhys. Lett.* **24** 665
[19] Xiong G M and Gong C D 1989 *Phys. Rev.* B **39** 9384
[20] Langer J S, Bar-On M and Miller H D 1975 *Phys. Rev.* A **11** 1417
[21] Jiang Z and Ebner C 1989 *Phys. Rev.* B **39** 2501

[22] Kawasaki K 1972 *Phase Transitions and Critical Phenomena* vol 2, ed C Domb and M S Green (New York: Academic) p 443 and references therein
[23] Binder K 1974 *Z. Phys.* B **267** 313
[24] Binder K and Frisch H L 1991 *Z. Phys.* B **84** 403
[25] Puri S and Binder K 1992 *Phys. Rev.* A **46** R4487
Puri S and Binder K 1994 *Phys. Rev.* E **49** 5359
[26] Hohenberg P C and Halperin B I 1977 *Rev. Mod. Phys.* **49** 435
[27] Schmidt I and Binder K 1987 *Z. Phys.* B **67** 369
[28] Puri S and Binder K 1992 *Z. Phys.* B **86** 263
[29] Puri S, Binder K and Frisch H L 1997 in preparation
[30] Weeks J D 1980 *Ordering in Strongly Fluctuating Condensed Matter Systems* ed T Riste (New York: Plenum) p 293
[31] Van Beijeren H and Nolden I 1987 *Structure and Dynamics of Surfaces II* ed W Schommers and P Blanckenhagen (Berlin: Springer) p 259
[32] Binder K 1983 *Phase Transitions and Critical Phenomena* vol 8, ed C Domb and J L Lebowitz (London: Academic) p 1
[33] Binder K and Hohenberg P C 1972 *Phys. Rev.* B **6** 3461
[34] Diehl H W 1986 *Phase Transitions and Critical Phenomena* vol 10, ed C Domb and J L Lebowitz (London: Academic) p 75
[35] Dietrich S 1988 *Phase Transitions and Critical Phenomena* vol 12, ed C Domb and J L Lebowitz (London: Academic) p 1
[36] Fisher M E 1984 *J. Stat. Phys.* **34** 667
Fisher M E 1986 *J. Chem. Soc. Faraday Trans.* **282** 1569
[37] Diehl H W and Janssen H-K 1992 *Phys. Rev.* A **45** 7145
[38] Puri S and Binder K 1994 *J. Stat. Phys.* **77** 145
[39] Bhattacharya A, Rao M and Chakrabarti A 1994 *Phys. Rev.* E **49** 524
[40] Brown G, Chakrabarti A and Marko J F 1994 *Phys. Rev.* E **50** 1674
[41] Brown G and Chakrabarti A 1994 *J. Chem. Phys.* **101** 3310
Brown G and Chakrabarti A 1995 *J. Chem. Phys.* **102** 1440
[42] Oono Y and Shiwa Y 1987 *Mod. Phys. Lett.* B **1** 49
[43] Ma W-J, Keblinski P, Maritan A, Koplik J and Banavar J R 1993 *Phys. Rev.* E **48** R2362
[44] Sagui C, Somoza A M, Roland C and Desai R C 1993 *J. Phys. A: Math. Gen.* **26** L1163
[45] Ohta T, Jasnow D and Kawasaki K 1982 *Phys. Rev. Lett.* **49** 1223
[46] Jones R A L and Kramer E J 1990 *Phil. Mag.* B **62** 129
[47] Puri S and Frisch H L 1993 *J. Chem. Phys.* **79** 5560
[48] Frisch H L, Nielaba P and Binder K 1995 *Phys. Rev.* E **52** 2848
[49] Oono Y and Puri S 1987 *Phys. Rev. Lett.* **58** 836
Oono Y and Puri S 1988 *Phys. Rev.* A **38** 434
Puri S and Oono Y 1988 *Phys. Rev.* A **38** 1542
Puri S and Oono Y 1988 *J. Phys. A: Math. Gen.* **21** L755
Puri S 1988 *Phys. Lett.* **134A** 205
Rogers T M, Elder K R and Desai R C 1988 *Phys. Rev.* B **37** 196
Chakrabarti A and Gunton J D 1988 *Phys. Rev.* B **37** 3798